

**Supplemental Information**

**Human motor units in microfluidic devices are impaired by *FUS* mutations and improved by HDAC6 inhibition**

**Katarina Stoklund Dittlau, Emily N. Krasnow, Laura Fumagalli, Tijs Vandoorne, Pieter Baatsen, Axelle Kerstens, Giorgia Giacomazzi, Benjamin Pavie, Elisabeth Rossaert, Jimmy Beckers, Maurilio Sampaolesi, Philip Van Damme, and Ludo Van Den Bosch**

## Supplemental Information

### Supplemental table of contents

**Figure S1.** Myotube fusion index, fluidic isolation in microfluidic device and optimization of co-culture protocol. Related to figure 1.

**Figure S2.** Agrin and laminin treatment enhance acetylcholine receptor clustering and NMJ formation. Related to Figure 3.

**Figure S3.** Agrin and laminin improve neurite outgrowth. Related to Figure 3.

**Figure S4.** Myotube functionality controls and *FUS*-ALS MN differentiation verification related to Figure 4-7.

**Figure S5.** NMJ images related to Figure 5.

**Figure S6.** Neurite outgrowth related to Figure 6.

**Figure S7.** Neurite outgrowth in mono-culture and *FUS* mislocalization. Related to Figure 5-7.

**Table S1.** Primary antibody overview. Related to Figure 1-3 and 5-7.

**Table S2.** Secondary antibody overview. Related to Figure 1-3 and 5-7.

**Table S3.** Neurite outgrowth thresholds. Related to Figure 6.

**Table S4.** Neurite regrowth thresholds. Related to Figure 6.

### Supplemental Experimental Procedures

### Supplemental References

**Figure S1**

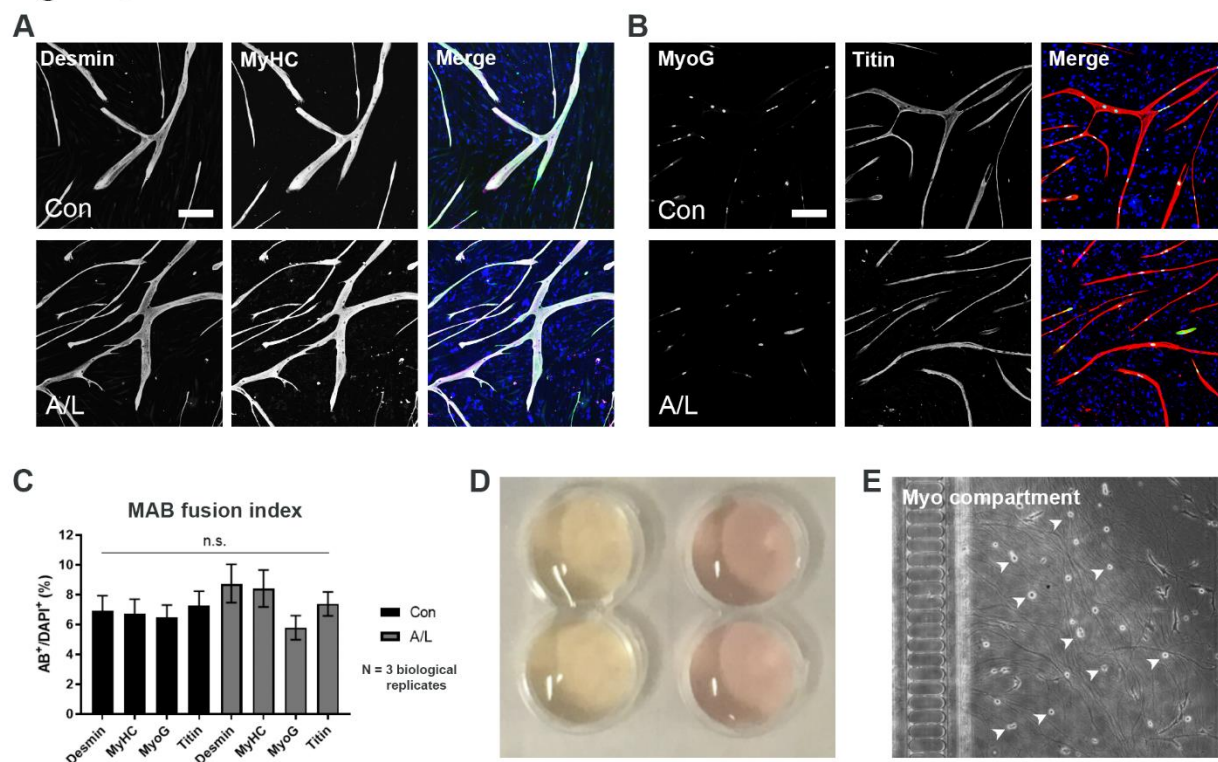


**Figure S1: Myotube fusion index, fluidic isolation in microfluidic device and optimization of co-culture protocol. Related to figure 1.**

**A-B.** Representative confocal images of myotube markers (AB<sup>+</sup>): desmin, myosin heavy chain (MyHC), myogenin (MyoG) and titin in agrin (0.01  $\mu$ g/ml) and laminin (20  $\mu$ g/ml) supplemented conditions (A/L) and untreated controls (Con) after 10 days of differentiation. **C.** Quantification of MAB's fusion into multinucleated myotubes (fusion index). Control data are identical to Figure 1.D. All data represent mean  $\pm$  s.e.m. of 3 biological replicates and statistical analysis in panel **C** was performed using one-way Anova and Tukey's multiple comparisons test. **D.** Confirmation of fluidic isolation between left and right compartments in an XC150 microfluidic device. By establishing a volumetric gradient, the pH-sensitive medium on the motor neurons changes colour to yellow (left side), whereas the medium in the empty compartment remains pink (right side) after 24 h. **E.** Maturation of MN in a device for 2 weeks (=day 24) before seeding of MABs (arrowheads). In order to prolong MN maturation and the sustainability of the co-culture system, we attempted to plate MABs at day 24 of MN differentiation. However, two weeks of MN maturation in the device resulted in large amounts of spontaneous neurite crossing, which inhibited the attachment of MABs in the channel (arrowheads). Due to the lack of myotube formation, we performed the seeding of MABs at day 17 (Figure 1.E).

Figure S2

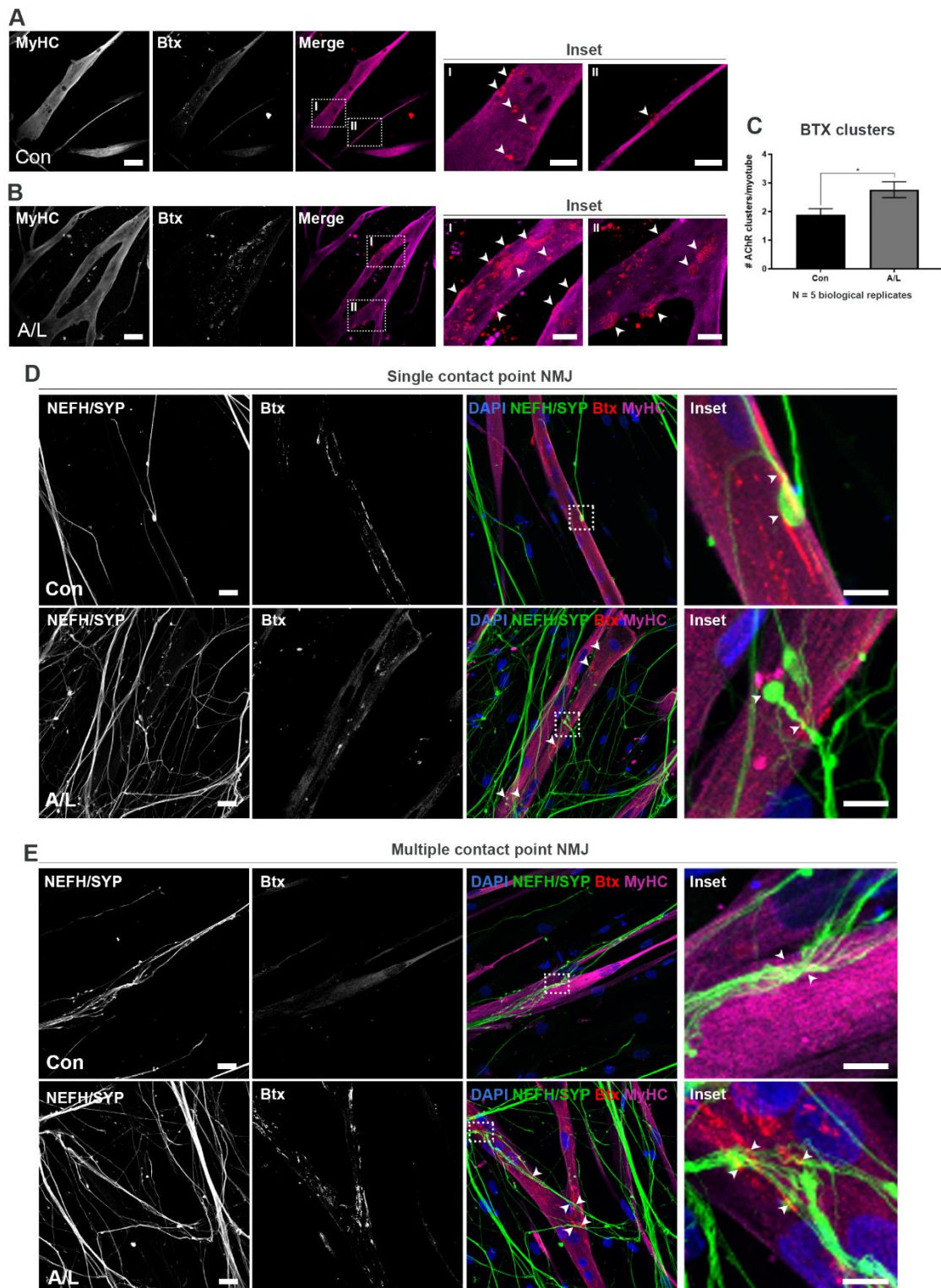


**Figure S2: Agrin and laminin treatment enhance acetylcholine receptor clustering and NMJ formation. Related to Figure 3.**

**A-B.** Representative ICC images of MyHC-positive myotubes with Btx-positive AChR clusters after 10 days differentiation in control conditions (Con) and with supplements of agrin and laminin (A/L). Scale bar: 75  $\mu$ m.

Insets represent a magnification of AChR clusters (arrowheads). Inset scale bar: 25  $\mu\text{m}$ . **C.** Quantifications of AChR cluster number per myotube. The data represent mean  $\pm$  s.e.m. of 3 biological replicates and statistical analysis was performed using unpaired t-test with  $*p < 0.05$ . **D-E.** Confocal micrographs of NMJs in agrin and laminin supplemented conditions (A/L) and untreated controls (Con) at 28 days of MN differentiation in XC150 microfluidic devices. NEFH- and SYP-positive motor neuronal axons either form a single contact point connection with myotubes forming rudimental NMJs (**D**) or they fan out upon interaction with myotubes and create multiple contact point NMJs (**E**). Scale bar: 25  $\mu\text{m}$ . Arrowheads mark co-localizations between SYP/NEFH and Btx. Inset scale bar: 10  $\mu\text{m}$ .



Figure S3

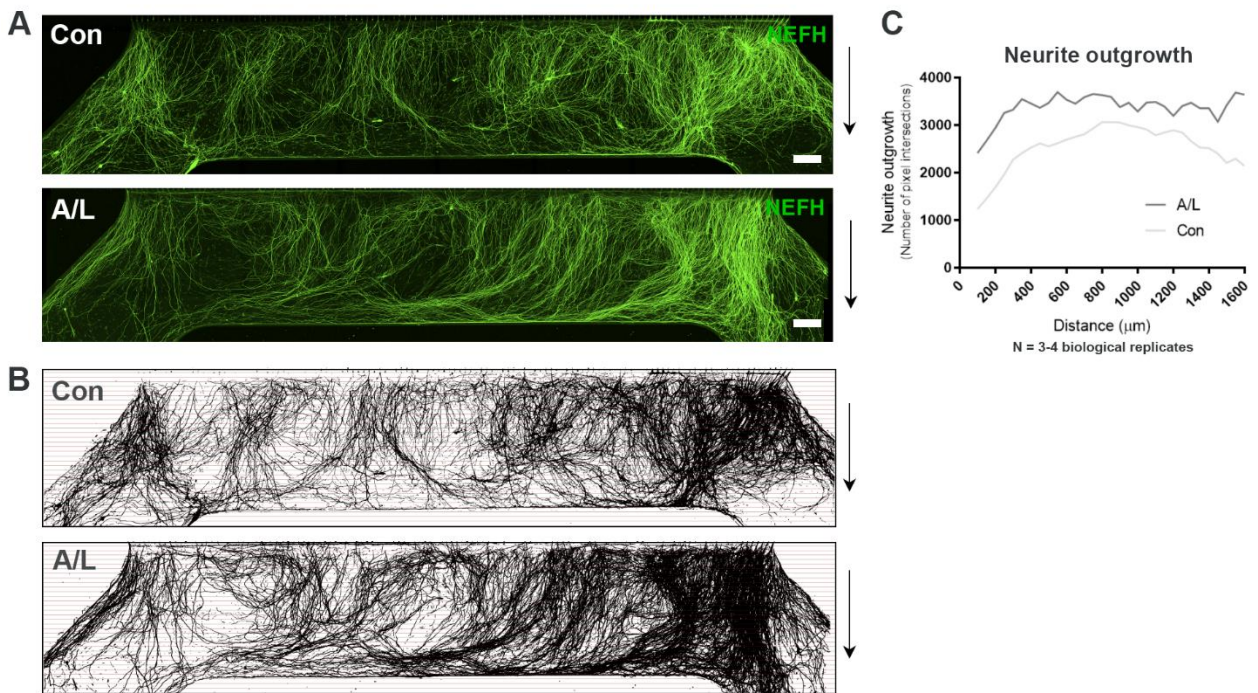


**Figure S3: Agrin and laminin improve neurite outgrowth. Related to Figure 3.**

**A.** Tile scan confocal overviews of neurite outgrowth in myotube compartment at day 28 of MN differentiation. Arrows (right) depict growth direction from exit of microgrooves. Scale bar: 300  $\mu\text{m}$ . **B.** Masks of tile scans with intersection lines at every 50  $\mu\text{m}$  from microgroove exit. **C.** Neurite outgrowth quantifications of the number of pixel intersections in each condition (A/L and Con). Panel **C** was performed in 3-4 biological replicates with mean graphs shown.

Figure S4

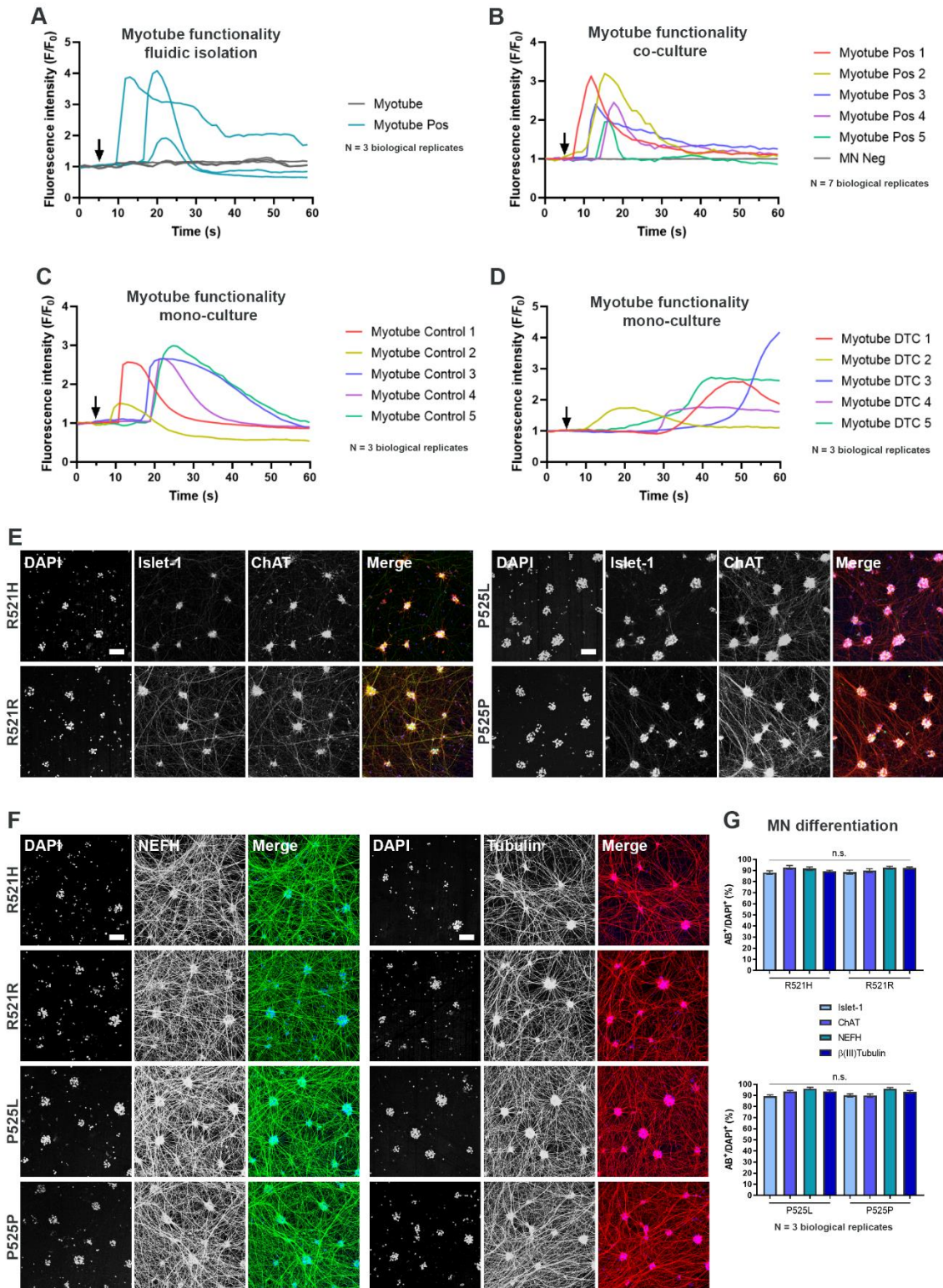


Figure S4. Myotube functionality controls and *FUS*-ALS MN differentiation verification related to Figure 4-7.

A. Representative  $Ca^{2+}$  influx curves in myotubes cultured in microfluidic devices without MNs in order to confirm fluidic isolation during KCl stimulation (arrow). The empty MN compartment was first stimulated with

50mM KCl (Myotube), followed by a direct KCl stimulation of myotubes in myotube compartment (Myotube pos). **B.** Representative  $\text{Ca}^{2+}$  influx curves in myotubes in co-culture with MNs after direct KCl stimulation (arrow) of myotubes in myotube compartment (Myotube Pos 1-5). MN Neg curve represent a recording of the MN compartment after MN stimulation with KCl confirming a fluidic isolation between compartments during incubation with the Fluo-4 dye. **C.** Representative  $\text{Ca}^{2+}$  influx curves in myotubes cultured without MNs. Arrow mark KCl stimulation. **D.** Representative  $\text{Ca}^{2+}$  influx curves in myotubes cultured without MNs after 10 min treatment with 19  $\mu\text{M}$  nicotinic AChR competitive antagonist tubocurarine. Arrow mark KCl stimulation. Data in **A** and **B** represents 3 and 7 biological replicates, respectively, while **C** and **D** represent 3 biological replicates with each three technical replicates. **E-F.** Confocal images of mutant *FUS* MNs (P525L, R521H) and isogenic control MNs (P525P, R521R). MNs are stained with MN markers Islet-1 and choline acetyltransferase (ChAT) (**E**) and neurofilament heavy chain (NEFH) as well as the pan-neuronal marker  $\beta$ III-tubulin (Tubulin) (**F**) at day 28 of MN differentiation. Scale bar: 75  $\mu\text{m}$ . **G.** Relative number of cells positive for MN and pan-neuronal markers. The data in panel **G** represent mean  $\pm$  s.e.m and statistical analysis was performed using Kruskal-Wallis test with Dunn's multiple comparisons test from 3 biological replicates.



Figure S5

A

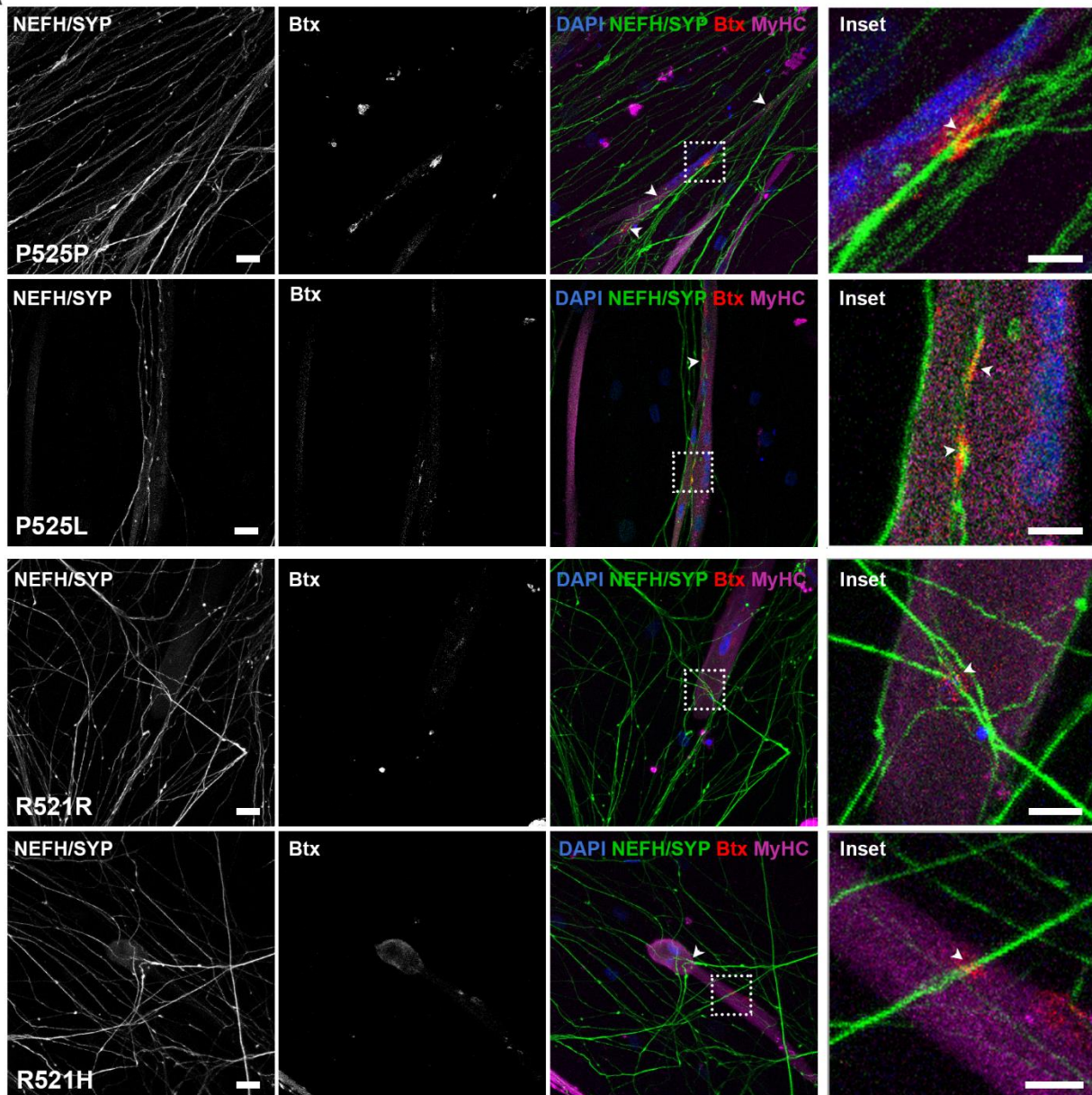


**Figure S5: NMJ images related to Figure 5.**

**A.** Confocal micrographs of NMJs in A/L supplemented conditions from *FUS*-mutant MN/myotube co-cultures (P525L, R521H) and isogenic control MN/myotube co-cultures (P525P, R521R) at 28 days of MN differentiation in XC150 microfluidic devices. Scale bar: 25  $\mu\text{m}$ . Arrowheads mark co-localizations between SYP/NEFH and Btx. Inset scale bar: 10  $\mu\text{m}$ .



Figure S6

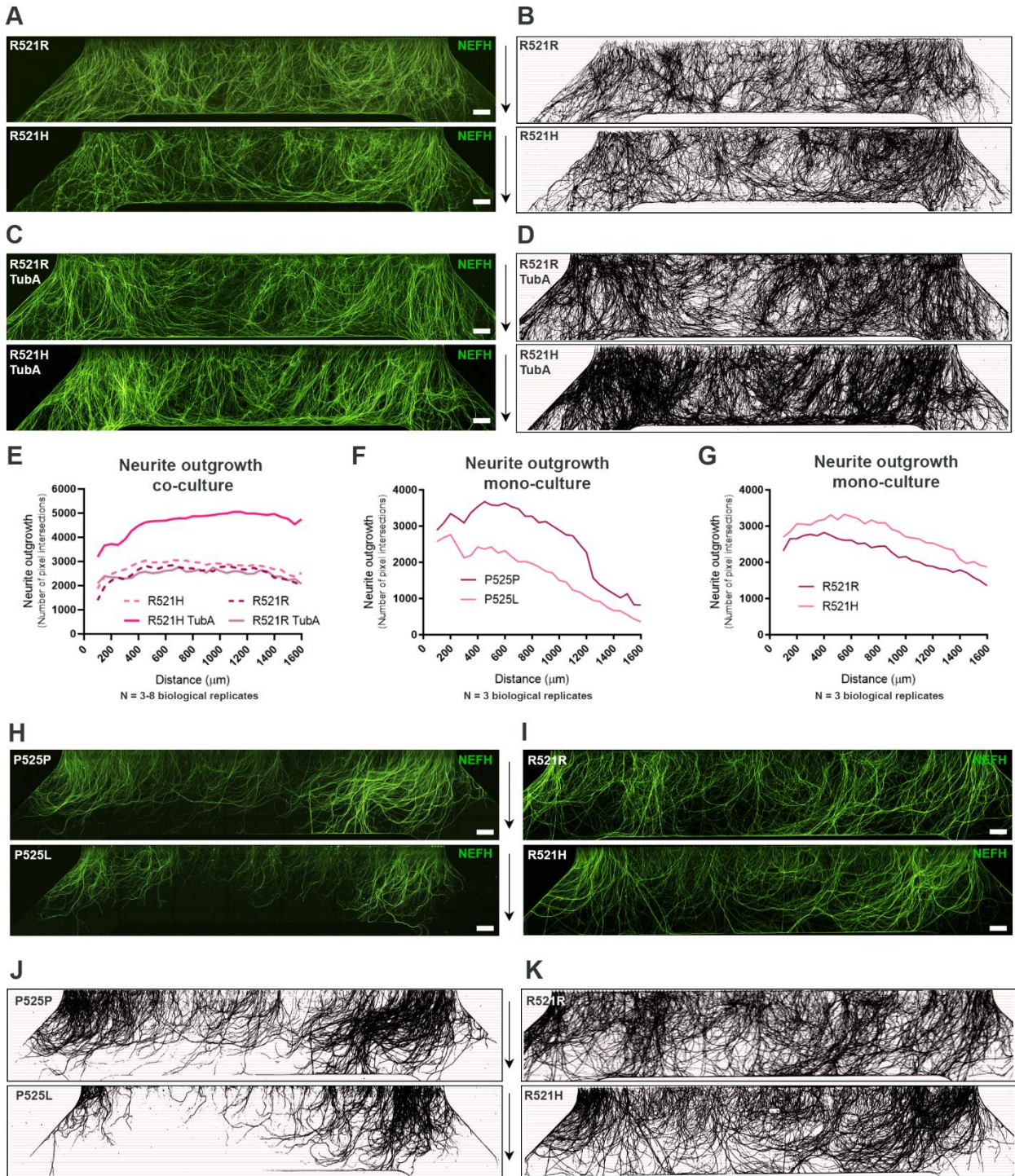


**Figure S6: Neurite outgrowth related to Figure 6.**

**A.** Tile scan confocal overviews of neurite outgrowth (NEFH) in myotube compartment from mutant *FUS* (R521H) and isogenic control (R521R) MN/myotubes co-cultures at day 28 of MN differentiation. Arrows (right) depict growth direction from exit of microgrooves. Scale bar: 300 µm. **B.** Masks of tile scans with intersection lines at every 50 µm from microgroove exit. **C.** Tile scan images of neurite outgrowth in R521R and R521H MN/myotube co-cultures after 24 h of Tubastatin A (TubA) treatment. Scale bar: 300 µm. **D.** Masks of tile scans with TubA treatment. **E.** Neurite outgrowth quantifications of pixel intersections in R521R and R521H MN/myotube co-cultures with and without treatment with TubA. **F-G.** Neurite outgrowth quantifications in

myotube compartment from mutant *FUS* (P525L, R521H) and corresponding isogenic controls (P525P, R521R) of the number of pixel intersections in MN cultures without myotubes. **H-J**. Tile scan confocal overviews of neurite outgrowth in MN cultures without myotubes. **J-K**. Masks of tile scans cultured without myotubes with intersection lines at every 50  $\mu\text{m}$  from microgroove exit. Data is from 3-8 biological replicates.



**Figure S7**

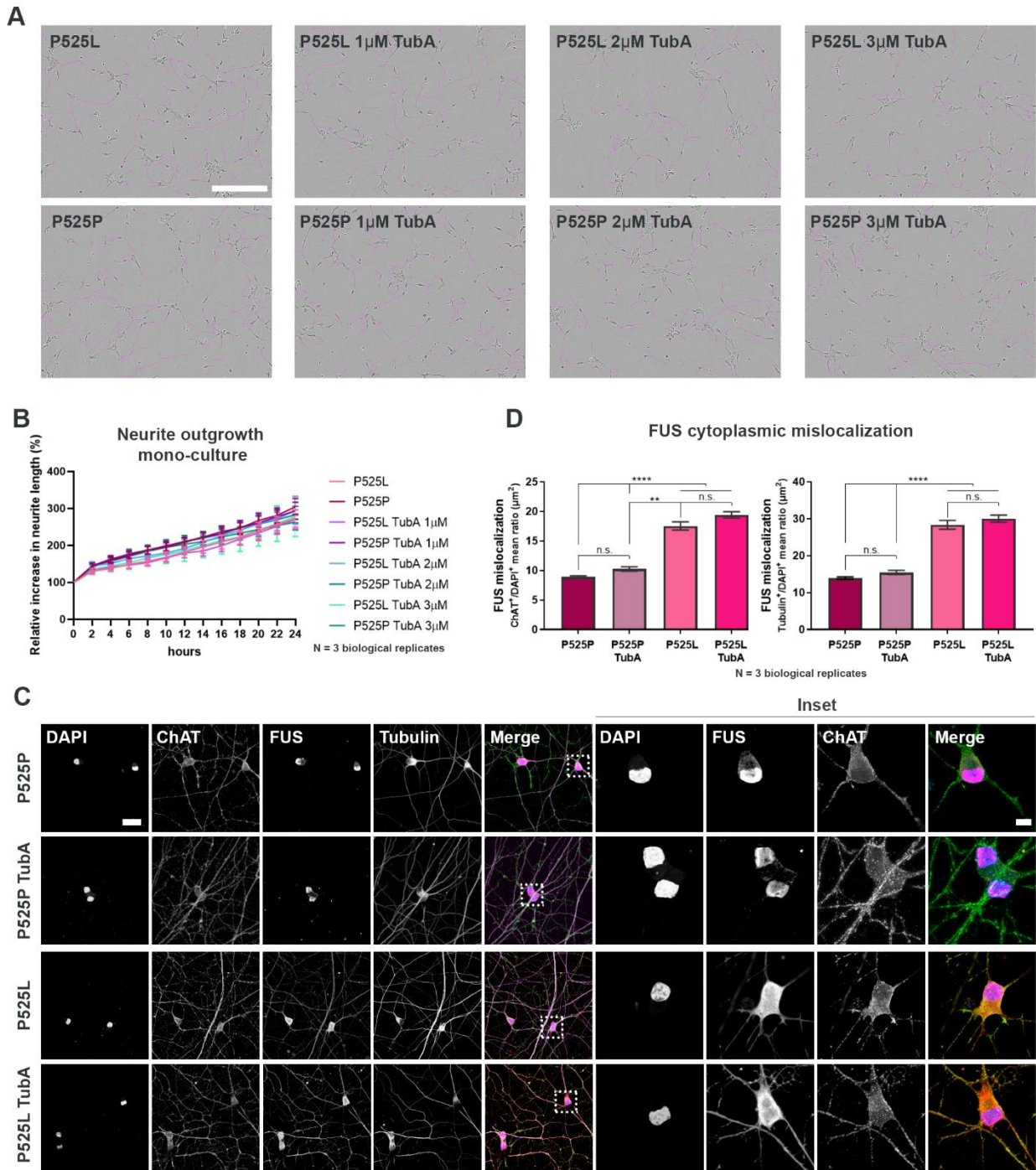


**Figure S7. Neurite outgrowth in mono-culture and FUS mislocalization. Related to Figure 5-7.**

**A.** Representative IncuCyte bright field images 24 h after plating of *FUS*-ALS patient line P525L and isogenic control P525P day 10 MN-NPCs with 1-3  $\mu$ M Tubastatin A (TubA) treatment and controls receiving no treatment. Neurite are marked using IncuCyte Phase Neurite mask. Scale bar: 200  $\mu$ m. **B.** Quantifications of relative increase in neurite length. Data represent mean  $\pm$  s.e.m and statistical analysis was performed using one-way Anova with Tukey's multiple comparisons test from 3 biological replicates with two technical replicates in each. **C.** Representative confocal micrographs of day 22 MNs from *FUS*-ALS patient line P525L and isogenic control P525P with and without 24h of 1  $\mu$ M TubA treatment. Treatment was initiated from day 21 to day 22 of

MN differentiation. Scale bar: 200  $\mu\text{m}$ . Inset: magnification of MN soma. Inset scale bar: 10  $\mu\text{m}$ . **D.** Quantifications of cytoplasmic/nucleus ratio of FUS. Data represent mean  $\pm$  s.e.m and statistical analysis was performed using one-way Anova with Tukey's multiple comparisons test or Kruskal-Wallis test with Dunn's multiple comparisons test from 3 biological replicates with two technical replicates in each. Outliers (Q=1%) were removed. \*\* $p < 0.01$  and \*\*\*\* $p < 0.0001$ .



**Table S1: Primary antibody overview. Related to Figure 1-3 and 5-7.**

Antibody	Dilution	Company	Antibody Identifier	Registry*
Rabbit anti-neurofilament heavy chain (NEFH)	1:1000	Abcam, Cat N° AB8135	AB_306298	
Rabbit anti-synaptophysin (SYP)	1:1000	Cell Signaling, Cat N° 5461S	AB_10698743	
Mouse anti-myosin heavy chain (MyHC)	1:20	In-house, SCIL		
Goat anti-choline acetyltransferase (ChAT)	1:500	Millipore, Cat N° ab144P	AB_2079751	
Rabbit anti-islet 1	1:400	Millipore, Cat N° ab4326	AB_10563961	
Mouse anti- $\beta$ III-tubulin	1:500	Abcam, Cat N° ab7751	AB_306045	
Mouse anti-titin	1:300	Developmental Studies Hybridoma Bank, Cat N° 9D10	AB_528491	
Rabbit anti-myogenin (MyoG)	1:500	Abcam, Cat N° Ab124800	AB_10971849	
Rabbit anti-desmin	1:200	Abcam, Cat N° Ab15200	AB_301744	
Rabbit anti-FUS/TLS	1:50	Proteintech, Cat N° 115701-AP	AB_2247082	

\* <https://antibodyregistry.org/>

**Table S2: Secondary antibody overview. Related to Figure 1-3 and 5-7.**

Antibody	Dilution	Company	Antibody Identifier	Registry*
Alexa Flour™ IgG (H+L) donkey-anti-rabbit	488 1:1000	Thermo Fisher Scientific, Cat N° A21206	AB_2535792	
Alexa Flour™ IgG (H+L) donkey-anti-goat	555 1:1000	Thermo Fisher Scientific, Cat N° A21432	AB_2535853	
Alexa Flour™ IgG (H+L) donkey-anti-mouse	555 1:1000	Thermo Fisher Scientific, Cat N° A31570	AB_2536180	
Alexa Flour™ IgG (H+L) donkey-anti-mouse	647 1:1000	Thermo Fisher Scientific, Cat N° A31571	AB_162542	
$\alpha$ -bungarotoxin (Btx) 555	Alexa Flour™ 1:1000	Thermo Fisher Scientific, Cat N° B35451	AB_2617152	

\* <https://antibodyregistry.org/>

**Table S3: Neurite outgrowth thresholds. Related to Figure 6.**

Sample ID (MN/Myotube co-cultures)	Threshold (%)	Sample ID (MN/Myotube co-cultures)	Threshold (%)	Sample ID TubA treatment (MN/Myotube co-cultures)	Threshold (%)
A/L biological replicate 1	60	R521H biological replicate 1	35	P525L biological replicate 1	50
A/L biological replicate 2	60	R521H biological replicate 2	70	P525L biological replicate 2	60
A/L biological replicate 3	70	R521H biological replicate 3	70	P525L biological replicate 3	55
A/L biological replicate 4	70	R521H biological replicate 4	30	P525P biological replicate 1	55
Control biological replicate 1	40	R521H biological replicate 5	50	P525P biological replicate 2	50
Control biological replicate 2	45	R521H biological replicate 6	50	P525P biological replicate 3	55
Control biological replicate 3	60	R521H biological replicate 7	50	R521H biological replicate 1	60
P525L biological replicate 1	40	R521H biological replicate 8	50	R521H biological replicate 2	50
P525L biological replicate 2	40	R521R biological replicate 1	50	R521H biological replicate 3	50
P525L biological replicate 3	45	R521R biological replicate 2	60	R521H biological replicate 4	60
P525L biological replicate 4	50	R521R biological replicate 3	50	R521H biological replicate 5	50
P525L biological replicate 5	45	R521R biological replicate 4	45	R521R biological replicate 1	30
P525L biological replicate 6	50	R521R biological replicate 5	35	R521R biological replicate 2	25
P525P biological replicate 1	70	R521R biological replicate 6	50	R521R biological replicate 3	50
P525P biological replicate 2	50	<b>Sample ID (MN without myotubes)</b>	<b>Threshold (%)</b>	<b>Sample ID (MN without myotubes)</b>	<b>Threshold (%)</b>
P525P biological replicate 3	60	P525L biological replicate 1	35	R521H biological replicate 1	50
P525P biological replicate 4	60	P525L biological replicate 2	35	R521H biological replicate 2	40
P525P biological replicate 5	50	P525L biological replicate 3	35	R521H biological replicate 3	30
P525P biological replicate 6	35	P525P biological replicate 1	35	R521R biological replicate 1	50
P525P biological replicate 7	55	P525P biological replicate 2	35	R521R biological replicate 2	50
		P525P biological replicate 3	35	R521R biological replicate 3	40

**Table S4: Neurite regrowth thresholds. Related to Figure 6.**

Sample ID Controls	Threshold (%)	Sample ID Pre-axotomy TubA treatment	Threshold (%)	Sample ID Post-axotomy TubA treatment	Threshold (%)
P525L biological replicate 1, technical replicate 1	25	P525L biological replicate 1, technical replicate 1	40	P525L biological replicate 1, technical replicate 1	50
P525L biological replicate 1, technical replicate 2	45	P525L biological replicate 1, technical replicate 2	20	P525L biological replicate 1, technical replicate 2	20
P525L biological replicate 2, technical replicate 1	15	P525L biological replicate 2, technical replicate 1	25	P525L biological replicate 2, technical replicate 1	15
P525L biological replicate 2, technical replicate 2	20	P525L biological replicate 2, technical replicate 2	25	P525L biological replicate 2, technical replicate 2	20
P525L biological replicate 3, technical replicate 1	15	P525L biological replicate 3, technical replicate 1	20	P525L biological replicate 3, technical replicate 1	20
P525L biological replicate 3, technical replicate 2	15	P525L biological replicate 3, technical replicate 2	20	P525L biological replicate 3, technical replicate 2	20
P525P biological replicate 1, technical replicate 1	35	P525P biological replicate 1, technical replicate 1	40	P525P biological replicate 1, technical replicate 1	50
P525P biological replicate 1, technical replicate 2	20	P525P biological replicate 1, technical replicate 2	50	P525P biological replicate 1, technical replicate 2	40
P525P biological replicate 2, technical replicate 1	20	P525P biological replicate 2, technical replicate 1	15	P525P biological replicate 2, technical replicate 1	20
P525P biological replicate 2, technical replicate 2	20	P525P biological replicate 2, technical replicate 2	15	P525P biological replicate 2, technical replicate 2	20
P525P biological replicate 3, technical replicate 1	15	P525P biological replicate 3, technical replicate 1	20	P525P biological replicate 3, technical replicate 1	20
P525P biological replicate 3, technical replicate 2	15	P525P biological replicate 3, technical replicate 2	20	P525P biological replicate 3, technical replicate 2	15

## Supplemental Experimental procedures

### Ethics

Healthy human control iPSCs (SBAD2 line) is derived by StemBANCC and was previously provided to SCIL by Dr. P. Jennings (Innsbruck University, Austria) as part of the EU-ToxRisk consortium (1). The CRISPR/Cas9 gene-edited isogenic controls (P525P and R521R) were generated by CellSystems (Troisdorf, Germany). iPSCs were transfected with gRNA vector, Cas9 vector, and donor DNA, and transfected cells were selected with puromycin for 2 days. Single clones were genotyped with genomic DNA PCR and subsequently sequenced, which confirmed the absence of the FUS mutations (2,3).

Written informed consent was obtained from the subjects who provided their samples for iPSC generation and MAB harvest. MAB isolation and characterisation was approved by the medical ethics committee of the University Hospital Leuven (n° S5732-ML11268). The generation of iPSCs from the healthy control was approved by the UK's main research ethics committee as part of the StemBANCC project, while the use of iPSC in this study was approved by the ethics committee of KU Leuven. The use of *FUS* patient fibroblasts and generation of iPSCs was approved by the ethics committee of the University Hospital Leuven (n° S50354 and S63792). All cells were routinely tested for mycoplasma contamination with MycoAlert Mycoplasma Detection Kit (Lonza, Rockland, ME, USA, Cat N° LT07-318).

### Preparation of microfluidic devices

Microfluidic devices (Xona™ Microfluidics, Temecula, CA, USA; Cat N° SND75 (microgroove length: 75 µm) and Cat N° XC150 (microgroove length: 150 µm)) and 7.8mil Aclar 33C sheets (Electron Microscopy Sciences, Hatfield, PA, USA, Cat N° 50425-25) were sterilized in 70% ethanol and left to air-dry in the laminar flow. Devices were placed individually in 10 cm petri dishes for easy handling. SND75 devices and Aclar sheets were coated separately using 100 µg/ml poly L-ornithine (PLO) (Sigma, St. Louis, MO USA, Cat N° P3655-100MG) in DPBS (Cat N° 14190250) prior to mounting of devices on the Aclar sheet. XC150 devices were coated directly using 100 µg/mL PLO in DPBS. Importantly, avoidance of air bubble formation was ensured during the coating of the channels by never removing liquid directly from channels.

All coated material was incubated at 37°C, 5% CO<sub>2</sub> for 3 h and subsequently washed twice in DPBS and once in sterile water. SND75 devices and Aclar sheets were left in the laminar flow cabinet for complete drying (20-30 min) before mounting of devices onto Aclar sheets. Assembly was performed in the laminar flow under a microscope with the use of a forceps to ensure the complete alignment of channels, grooves and borders of the wells. Once assembled, devices were checked for leakage and coated with 20 µg/ml laminin (Sigma, Cat N° L2020-1MG) in Neurobasal medium (Cat N° 21103049). A volume difference was established between the two sides of the device to allow laminin coating to pass through the microgrooves and the devices were incubated overnight at 37°C in 5% CO<sub>2</sub>. Overnight incubation hardened the silicone SND75 devices and further sealed them onto the Aclar sheets. The following day, devices were carefully flushed once with DPBS before plating neural progenitor cells (NPCs).

### Differentiation of iPSCs into motor neuronal progenitor cells and seeding in microfluidic device

In brief, iPSCs were harvested using collagenase type IV (Cat N° 10780004) and collected in Corning® ultra-low attachment flasks (Sigma, Cat N° 734-4140) to facilitate embryoid body formation. Cells were maintained in neuronal medium (50% DMEM/F12 (Cat N° 11330032) and 50% Neurobasal medium (Cat N° 21103049) with 0.5% L-glutamine (Cat N° 25030-024), 1% penicillin/streptomycin (Cat N° 15070063), 1% N-2 supplement (Cat N° 17502-048), 2% B-27™ without vitamin A (Cat N° 12587-010), 0.5 µM ascorbic acid (Sigma, Cat N° A4403), and 0.1% β-mercaptoethanol (Cat N° 31350010)) supplemented with 5 µM Y-27632 (Merck Millipore, Burlington, MA, USA; Cat N° 688001), 0.2 µM LDN-193189 (Stemgent, Beltsville, MA, USA; Cat N° 04-0074-02), 40 µM SB431542 (Tocris Bioscience, Bristol, UK, Cat N° 1614) and 3 µM CHIR99021 (Tocris Bioscience, Cat N° 4423) for 2 days with medium changes every day (=day 0-1). The following day (=day 2), neuronal medium was supplemented with 0.1 µM retinoic acid (Sigma; Cat N° R2625) and 500 nM smoothened agonist (Merck Millipore; Cat N° 566660), which was refreshed at day four. On day 7, 10 ng/ml BDNF (Peprotech, Rocky Hill, NJ, USA, Cat N° 450-02B) and 10 ng/ml GDNF (Peprotech, Cat N° 450-10B) was additionally added to the day four medium. On day 9, 20 µM DAPT (Tocris Bioscience, Cat N° 2634) was additionally supplemented to day 7 medium. On day 10, embryoid bodies were dissociated into a single cell NPC suspension using 0.05% trypsin (Gibco, Gaithersburg, MA, USA, Cat N° 25300054) and cryopreserved. NPCs were seeded in the two wells and channel on one side of the microfluidic device at 125,000 cells in 30-50 µl day nine medium supplemented with 1% RevitaCell™ (Cat N° A2644501) per well (total of 250,000

NPCs/device). After seeding, devices were incubated for 5-10 min at 37°C and 5% CO<sub>2</sub> to allow cell attachment to the surface before additional day nine medium was added to all 4 wells for a total of 200 µl/well. Subsequently, 5-6 ml sterile DPBS was added to the 10 cm petri dish around the devices to avoid medium evaporation. Seeding in both wells and channel facilitated a larger and more robust network of MNs, which was less likely to detach during medium changes.

### **Derivation and maintenance of human mesoangioblasts**

Briefly, upon receipt of skeletal muscle biopsy, the tissue was minced and incubated for 2 weeks on collagen from calf skin-coated (Cat N° 17104019) 6-cm dishes in growth medium: 15% FBS (Cat N° 10270106), 1% sodium pyruvate (Life Technologies, Carlsbad, CA, USA, Cat N° 11360-070), 1% non-essential amino acids (Cat N° 11140050), 1% L-glutamine (Cat N° 25030-024), and 0.5% penicillin-streptomycin (Cat N° 15070063), and 1% insulin transferrin selenium (Cat N° 41400045) in IMDM (Cat N° 12440053) supplemented with 5 ng/ml recombinant human basic fibroblast growth factor (bFGF) (Peprotech, Cat N° 100-18B). Medium was changed every 4 days. After 14 days, cells were fluorescent activated cell (FACS)-sorted for human alkaline phosphatase (R&D systems, Minneapolis, MN, USA, Cat N° MAB1448) and expanded further in T75 flasks (Sigma, Cat N° CLS3276) on collagen from calf skin (Cat N° 17104019) in growth medium. Cells were cryopreserved in knockout serum replacement (Cat N° 10828-028) with 10% DMSO (Sigma, Cat N° D2650-100ML), passaged, or seeded in devices when reaching 70% confluence. For passaging MABs were washed once with DPBS, followed by incubation with TrypLE express (Cat N° 12605010) for 3 min at 37°C in 5% CO<sub>2</sub>. After incubation, TrypLE was neutralized with growth medium, and cells were gently scraped, collected and centrifuged for 3 min at 0.3 RCF, before cells were counted and reseeded in a T75 or T175 flask or device. Passaging was performed 1-2 times a week for cell expansion until a maximum passage number of 13. Since physical contact between MABs initiates fusion and lowers the myogenic potential, a cell confluence of 70% was never exceeded.

### **Co-culturing myotubes and motor neurons in microfluidic device**

On day 11 of motor neuron differentiation, day 10 medium was refreshed on both sides of the device keeping an equal volume across microgrooves. On day 14, 200 µl neuronal medium supplemented with 10 ng/ml BDNF, 10 ng/ml GDNF and 20 µM DAPT was added to each well to initiate NPC differentiation into spinal MNs (sMNs). On day 16, 200 µl day 14 medium additionally supplemented with 10 ng/ml CNTF (Peprotech, Cat N° 450-13B) was added to each of the four wells. On day 17, MABs were dissociated using TrypLE and seeded in the two wells and channel opposite to the MNs in the microfluidic device at 100,000 cells in 30-50 µl growth medium per well (total of 200,000 MABs/device). After seeding, devices were incubated for 5-10 min at 37°C in 5% CO<sub>2</sub> to allow cell attachment to the surface before additional growth medium was added to the two wells for a total of 200 µl/well. MABs were large cells with spherical morphology when dissociated in suspension. On day 18, MN compartments received neuronal medium supplemented with 10 ng/ml BDNF, GDNF and CNTF, while MABs differentiation into myotubes was initiated in the opposite compartments using MAB differentiation medium containing 2% horse serum (Cat N° 16050122) and 1% sodium pyruvate in DMEM/F12 supplemented with 0.01 µg/ml recombinant human agrin protein (R&D Systems, Cat N° 6624-AG-050). At day 21, a 300% chemotactic growth factor gradient and 200% volumetric gradient were established to facilitate polarized axonal growth through the microgrooves of the microfluidic device towards the myotube compartment. MN compartments received 100 µl/well neuronal medium without neurotrophic factor supplements, while myotube compartments received 200 µl/well neuronal medium supplemented with 30 ng/ml BDNF, GDNF and CNTF in addition to 20 µg/ml laminin and 0.01 µg/ml agrin. The growth factor and volume gradients including laminin and agrin supplements were kept at each medium change, which was performed every other day until day 28 of MN differentiation equivalent to 10 days of co-culturing MNs and myotubes. A spontaneous crossing of neurites from the MN soma compartment towards the myotube compartment without implementation of the chemotactic and volumetric gradient is generally observed. However, with the gradient the amount of neurites crossing and the speed of which this happens are increased.

### **Tubastatin A treatment**

For neurite outgrowth and NMJ quantifications, *FUS*-ALS and isogenic control co-cultures in XC150 devices were treated for 24 h with 1 µM Tubastatin A (TubA) (Selleckchem, Houston, TX, USA, Cat N° S8049) in day 21 medium in combination with the start of the chemotactic and volumetric gradient. TubA was added to both the soma and the myotube compartment. Control co-culture devices were kept in parallel without TubA treatment. At day 28, devices were analysed for neurite outgrowth and NMJ were quantified.



For neurite regrowth, *FUS*-ALS and isogenic control MNs were treated with 1 $\mu$ M TubA in both compartments for 24 h before (pre-axotomy) or for 24 h after (post-axotomy) performing the axotomy. Control devices were kept in parallel without TubA treatment.

For MN *FUS*-mislocalisation experiments, MNs were plated in 24-well plates (Greiner bio-one cellstar, Vilvoorde, Belgium, Cat N° 662160) and treated with 1 $\mu$ M TubA for 24 h from day 21-22, before subsequent fixation and analysis. Untreated controls were kept in parallel.

### **Immunocytochemistry**

Xona™ XC150 devices were used for immunocytochemistry (ICC) analysis of NMJ formation and neurite outgrowth, while MN differentiation verification, myotube fusion and MN *FUS*-mislocalisation were imaged on 13 mm #1.5 coverslips (VWR, Monroeville, PA, USA, Cat N° 631-0150P) and in 96-well black tissue culture plates (Perkin Elmer, Waltham, MA, USA, Cat N° 6005430). Cells were washed once with DPBS before fixation using 2-4% paraformaldehyde (Cat N° 28908) for 15-20 min at room temperature (RT). After fixation, cells were permeabilized for 20 min at RT with DPBS + 0.1% Triton X-100 (Sigma, Cat N° T8787-250ML) followed by blocking for 20 min at RT in 5% normal donkey serum (Sigma, Cat N° D9663-10ML) in 0.1% PBS-Triton X-100. Primary antibodies (table S1) were diluted in 0.1% PBS-Triton X-100 with 2% normal donkey serum and incubated with a volume gradient between MN/myotube compartments overnight at 4°C.

The following day, cells were carefully washed and incubated with secondary antibodies (table S2) diluted in 2% normal donkey serum in 0.1% PBS/Triton X-100 for 1h at RT in the dark with a volume gradient between compartments.

To label nuclei, cells were incubated with DAPI (NucBlue Live Cell Stain ReadyProbes reagent, Cat N° R37605) for 20 min and coverslips were mounted with Fluorescence Mounting Medium (Dako, Glostrup, Denmark, Cat N° S3023), while wells in the device were sealed with one drop of mounting medium per well before acquiring images. Coverslips, plates and devices were imaged using an inverted Leica SP8 DMI8 confocal microscope and quantifications were performed utilizing Image J 1.52b software.

For MN quantifications, a minimum of 100 cells were randomly selected based on positive DAPI staining. Five random images at 20x magnification were acquired from each biological replicate. For myotube fusion index, nuclei were counted using Image J particle analyser tool with a nucleus size between 50-700  $\mu$ m<sup>2</sup>. Five random images at 10x magnification were acquired from each biological replicate from each condition. For AChR cluster quantifications, a minimum of 20 random field of visions (=581.8  $\mu$ m<sup>2</sup>) per condition were selected and myotubes was determined based on positive myosin heavy chain (MyHC) marker. MyHC-positive cells containing multiple nuclei were selected as myotubes. For NMJ quantifications, each image field was selected based on  $\alpha$ -bungarotoxin (Btx)-positive clustering, recorded in z-stack, and the number of co-localizations between synaptophysin (SYP) and Btx was counted per myotube. For quantifying *FUS*-mislocalisation in MNs, eight random images at 12-bit and 40x magnification were taken blinded from two technical replicates from each biological replicate per condition. Images were converted to maximum intensity projection, and the nucleus/cytoplasmic ratio of *FUS* was quantified using a customised automatic Nikon software script.

### **Scanning electron microscopy**

For SEM, myotubes and motor neurons were cultured in Xona SND75 devices on Aclar sheets and fixed with 2.5% glutaraldehyde in 0.1 M Na-cacodylate buffer pH 7.2 for 2 h at RT. After three washing steps in the same buffer, the microfluidic devices were carefully removed and Aclar sheets were clipped to round discs of 18 mm diameter. Subsequently, the discs were incubated in 1% osmium tetroxide for 1 h, washed in milli-Q water and dehydrated in a graded ethanol series to 100% ethanol. The discs were then inserted in a coverslip-holder for critical point drying in a Leica CPD300 apparatus for two hours, in which they were kept submerged in 100% ethanol at all times. Finally, the dried discs were mounted on SEM support stubs with carbon-stickers and coated with 4 nm Chromium in a Leica ACE600 coating machine. Cells and myotubes were studied and imaged in a Zeiss Sigma SEM at an accelerating voltage of 5 kV and at a working distance of 7 mm.

### **Neurite axotomy and regrowth**

*FUS*-ALS and isogenic control MNs were cultured without myotubes in XC150 devices until day 22 according to our protocol. On day 22, the myotube compartment containing neurites was repeatedly washed from both channel openings with at least 2 ml DPBS and removed using suction in order to mechanically axotomize the neurites (4,5). This was followed by a 15 sec incubation with 100  $\mu$ l of lysis buffer (2% Triton X-100 (Sigma, Cat N° T8787-250ML) in DPBS) in order to chemically dissolve the remaining tissue. A volume difference between compartments with a higher volume on the MN soma side was maintained during the entire axotomy procedure to minimize the flow back of lysis buffer through the grooves. Afterwards, the lysis buffer was removed and the compartment was again repeatedly washed with DPBS before adding fresh MN medium to

the entire device and restoring the chemotactic and volumetric gradient. Devices were fixed at day 23 to allow the neurites to regrow for 24 h.

### **Neurite outgrowth and regrowth quantifications**

The co-cultures used for NMJ quantification were likewise used for neurite outgrowth quantifications. In addition, MNs cultured in devices without myotubes were used to assess a potential myotube influence on neurite outgrowth as well as assess neurite regrowth upon axotomy. Tile scan images of NEFH fluorescence were taken at 10x magnification in a 1024x1024 format using an inverted Leica SP8 DMI8 confocal microscope. Tile scans were merged automatically using Leica software auto merge and auto stitching with a smooth overlap and linear blending. Afterwards, images were cropped at the microgroove edge displaying solely the myotube compartment with crossing neurites. Neurites were identified and isolated using ilastik 1.3.3post1 Pixel Classification software with a sigma of 0.3-1.6 for color/intensity, edge and texture. The outlined neurites were exported as probabilities predictions. Each image was adjusted for a threshold between 15-70 % (see table S3 and table S4 for exact values) and converted to an 8-bit mask using Image J 1.52p software. Using Image J software's particle remover plugin, pixels between 0-10  $\mu\text{m}^2$  were removed. To assess neurite outgrowth and regrowth, total number of pixel intersections were quantified utilizing a custom-made Image J 1.52p software script. The script performs a linear Scholl analysis and automatically quantifies the amount of pixel crossings per line intersection similar to a previously published method (6). The distance between each line intersection is 50 $\mu\text{m}$ . Due to high neurite density and bundle formation at the exit of the microgrooves, we omitted the measurements at the first line at 50  $\mu\text{m}$  and started measuring at 100 $\mu\text{m}$  distance from the microgrooves.

For MN-NPC neurite outgrowth quantifications in mono-cultures, day 10 NPCs were plated in 24-well plates and imaged for 24 h using an IncuCyte ZOOM device with the IncuCyte ZOOM 2016A software and a Nikon S Plan Fluor ELWD 20X/0.45 OFN22 DIC N1 objective (Essen BioScience). Nine images per condition were taken every two hours. Cells were treated with 1-3  $\mu\text{M}$  TubA for 24 h with control conditions receiving no treatment. Neurite outgrowth was analysed using the IncuCyte NeuroTrack Phase Neurites software with a brightness segmentation mode, a segmentation adjustment of 1, a cleanup min cell width of 10  $\mu\text{m}$ , a neurite sensitivity of 0.5  $\mu\text{m}$  and neurite width of 1  $\mu\text{m}$ . The experiment was performed in three independent replicates with two technical replicates in each.

### **Calcium fluorescent imaging**

Xona™ XC150 devices were used for live-cell functionality assessment of NMJs. On day 28 of MN differentiation, myotube compartments were incubated for 25 min at 37°C, 5% CO<sub>2</sub> with 200  $\mu\text{l}$ /well neuronal medium supplemented with 30 ng/ml BDNF, GDNF and CNTF and 5  $\mu\text{M}$  Fluo-4 AM (Cat N° F14201) diluted in Pluronic F-127 (Cat N° P3000MP), while MN compartments received a medium change with 200  $\mu\text{l}$ /well neuronal medium without neurotrophic factors. Fluo-4 AM is a Ca<sup>2+</sup> indicator, which exhibits an increase in fluorescence upon Ca<sup>2+</sup> binding. After incubation, the medium was refreshed on both sides in order to re-establish the volume and growth factor gradient. MNs were stimulated with 50 mM potassium chloride (KCl) in neuronal medium and the consequent Fluo-4 fluorescence was recorded in the myotube compartment (10x magnification with 1 s intervals for a duration of 1 min per set). Each field of vision was selected with bright field based on the presence of myotubes in the myotube compartment. For each device, the motor neuron stimulation was performed twice with approximately 2 min pause in between, followed by a positive test of myotube activity with direct stimulation of myotubes with 50 mM KCl in myotube compartment. MN compartment was stimulated once to confirm fluidic isolation and absence of Fluo-4 AM flow back through microgrooves during incubation. In addition, myotubes were cultured without MNs in 24-well black ibitreat  $\mu$ -plates (Ibidi, Planegg, Germany, Cat N° 82406) and tested for Ca<sup>2+</sup> functionality, as well as in devices without MNs to confirm fluidic isolation upon KCl stimulation in the MN compartment. To guarantee the specificity of our experiment, myotube compartments were treated with 19  $\mu\text{M}$  of the AChR competitive antagonist tubocurarine hydrochloride pentahydrate (DTC) (Sigma, Cat N° T2379-100G) 10 min before analysis. All recordings were acquired and analysed with a Nikon A1R confocal microscope and NIS-Elements AR 4.30.02 software. For functionality quantifications, each myotube was manually circled utilising NIS-elements Time Measurement tool and individually analysed for increase in Fluo-4 fluorescent signal over a 1-min time period. Increase in Ca<sup>2+</sup> intensity was calculated as difference between peak value within first 30 recorded seconds and baseline. Baseline was calculated as average value of the first 5 seconds of recordings before KCl stimulation.

## Statistics

A biological replicate represents an independent MN differentiation from day 0 to day 28, and independent MAB differentiation into myotubes or an independent co-culture in a device. MN, myotube fusion index and AChR cluster quantifications were performed in three biological replicates, and NMJ quantifications in a total of four replicates with two technical replicates in each. NMJ functionality experiments were performed in four independent co-culture replicates and each experiment was performed in three technical replicates. NMJ blocking experiments with DTC were performed in three replicates. Neurite outgrowth quantifications were performed in three-four replicates using the healthy control iPSC line. For the *FUS*-iPSC lines, NMJ and neurite outgrowth quantifications were performed in three-eight replicates, and for TubA treatment in three-five replicates. Neurite regrowth and *FUS*-mislocalisation quantifications were done in three replicates with two technical replicates in each experiment. Outliers ( $Q=1\%$ ) were removed in the *FUS*-mislocalisation analysis.

## Supplemental References

1. Terryn J, Welkenhuysen M, Krylychkina O, Firrincieli A, Andrei A, Reumers V, et al. Topographical guidance of PSC-derived cortical neurons. *J Nanomater.* 2018;5238901.
2. Guo W, Naujock M, Fumagalli L, Vandoorne T, Baatsen P, Boon R, et al. HDAC6 inhibition reverses axonal transport defects in motor neurons derived from *FUS*-ALS patients. *Nat Commun.* 2017;8(1):861.
3. Wang H, Guo W, Mitra J, Hegde PM, Vandoorne T, Eckelmann BJ, et al. Mutant *FUS* causes DNA ligation defects to inhibit oxidative damage repair in Amyotrophic Lateral Sclerosis. *Nat Commun.* 2018;9:3683.
4. Nijssen J, Aguila J, Hoogstraaten R, Kee N, Hedlund E. Axon-Seq Decodes the Motor Axon Transcriptome and Its Modulation in Response to ALS. *Stem Cell Reports.* 2018;11:1565–78.
5. Nijssen J, Aguila J, Hedlund E. Axon-seq for in Depth Analysis of the RNA Content of Neuronal Processes. *Bio-Protocol.* 2019;9(14):1–16.
6. Jocher G, Mannschatz SH, Offterdinger M, Schweigreiter R. Microfluidics of small-population neurons allows for a precise quantification of the peripheral axonal growth state. *Front Cell Neurosci.* 2018;12:166.